Hindawi
Mathematical Problems in Engineering
Volume 2019, Article ID 3943472, 11 pages
https://doi.org/10.1155/2019/3943472

Research Article

Modeling and Speed Control of the Underwater Wheeled Vehicle Flexible Towing System

Gang Liu,[1] **Guohua Xu**,[1] **Guanxue Wang**,[1] **Guoqiang Yuan**,[2] **and Jiajia Liu**[1]

[1]*School of Naval Architecture and Ocean Engineering, Huazhong University of Science and Technology, Wuhan 430074, China*
[2]*Ocean Smart Technology Co., Ltd., Wuhan 430074, China*

Correspondence should be addressed to Guohua Xu; hustxu@vip.sina.com

Received 20 September 2018; Accepted 2 January 2019; Published 15 January 2019

Academic Editor: Luca Pugi

Copyright © 2019 Gang Liu et al. This is an open access article distributed under the Creative Commons Attribution License, which permits unrestricted use, distribution, and reproduction in any medium, provided the original work is properly cited.

In this paper, the research contents are mainly focused on the technology of the underwater wheeled vehicle speed control. For providing a passive towed underwater wheeled vehicle with accelerating, uniform motion and decelerating capability which can simulate an underwater navigation environment for the carried unit, we devised a novel open-type hydraulic flexible towing system. Combining the hydrodynamic model of the vehicle and the hydraulic mechanism model, the dynamic characteristics of the novel towing system are studied by computing simulation. Aiming at the force coupling character of double driving hydraulic winches, a master-slave synchronization control strategy is proposed. Then, in view of the flexible towing system features, i.e., strong coupling, nonlinear, time-varying load, and environmental constraints, a real speed controller based on fast terminal sliding mode control theory is designed and manufactured. To verify the effectiveness of the controller, a hardware-in-the-loop simulation test is carried out on the strength of a semiphysical simulation platform based on Matlab/Simulink and VxWorks real-time system. The experiment results show that the speed controller based on fast terminal sliding mode control has excellent effect on rapidity, stability, and anti-interference characteristics.

1. Introduction

In the new century, facing various challenges, especially in the global population, resources, and environment, people will inevitably pay more and more attention to sea and depend on the ocean. With the extensive research and development of the special equipment for marine resources exploitation and marine environmental detection, the related testing device is also developed rapidly [1–3]. The underwater wheeled vehicle flexible towing system presented in this paper is a new kind of experiment establishment which was built in a shallow water tank. The experiment system is mainly composed of a wheeled vehicle and a submersible lifting platform which can hover at the specified depth underwater and adjust the inclination of the platform itself by the using of intake and drainage system and lifter winches. With the help of the pulleys fixed on the lifting platform and the wire rope, the underwater wheeled vehicle can be towed to achieve steady horizontal uniform navigation on the track mounted on the surface of the lifting platform. If this experiment system is built in shallow seas, it can simulate a deeper and more realistic marine environment for the tested object. On account of this function, the underwater wheeled vehicle towing system can be applied to a variety of underwater applications, for example, providing a required-speed running environment, testing the dynamic performance of sensors and tested objects, capturing the tested equipment status data, and achieving effective data remote real-time transmission. We can find that the accurate and steady speed of the wheeled vehicle is the key to complete underwater dynamic testing.

Taking into consideration the fact that the hydraulic winch features higher efficiency and superior load capacity and is more economical than the electric winch, we choose the hydraulic valve control motor driving winch in this study [4]. As shown in Figure 1, the underwater wheeled vehicle towing system consists of an anterior traction winch, a posterior brake winch, track, wire rope, and fixed pulleys. The track is mounted on the surface of the lifting platform, and the two driving winches are, respectively, arranged on both ends of the track. Along the pulley group, the open-type hydraulic

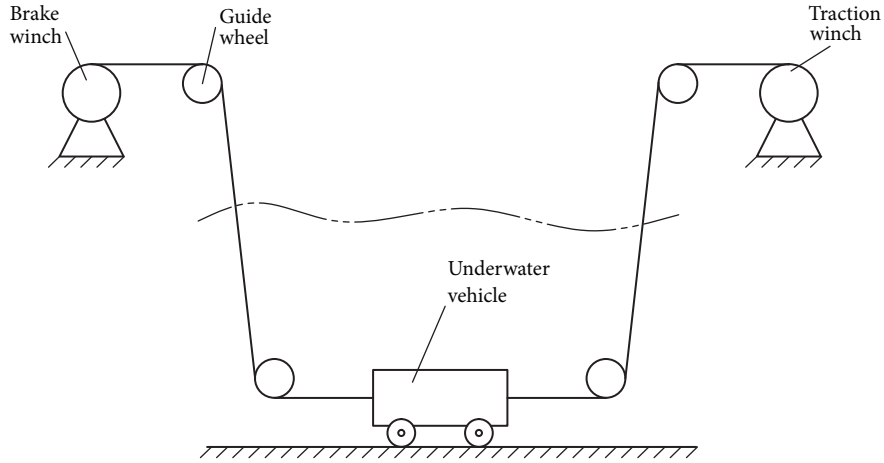

Figure 1: Schematic diagram of underwater vehicle propelled by hydraulic winch.

flexible towing system is linked by two ropes which are fixed and wound on the traction winch and brake winch. Driven by two winches, the vehicle can move horizontally on the track.

When the loaded underwater wheeled vehicle runs in a cuboid boundary pool, the complex water resistance will come from the fluid-structure interaction, wave-making interaction, and pond wall effect. In addition to this, there are uncertain parameters in hydraulic system and environment. So as to achieve the favorable and stabilized properties of sailing when the loaded wheeled vehicle is conducting a test, the speed controller must be provided with self-adaptive and robust property. As we all know, once the rope slackens, the tensile force becomes zero. If the speed of the vehicle is fluctuating, the wire rope will oscillate up and down, which will make the towing system destabilized or even destroyed. In order to avoid overlarge tension shock of the hinder rope, it is indispensable to put forward a multimode synchronous control strategy.

In modern times, many scholars have done plenty of research work on the modeling of hydraulic and fluid systems with rope actuation [5, 6] and proposed a good deal of advanced control technology such as feedback, neural network, adaptive robust control, and predictive control [7–11]. In order to predict the vibration characteristics of the armature assembly, Peng et al. focused on the mathematical modeling of the vibration characteristics of armature assembly in a hydraulic servo valve and the identification of parameters in the models [12]. Chen et al. developed the dynamic model of the valve-controlled hydraulic winch by linearizing its nonlinear dynamics at an operating point and found that the FUZZY P + ID controller is much more robust than the conventional PID controller [13]. Wei et al. demonstrated that the nonlinear cascade controller together with the extended fuzzy disturbance observer provides an excellent motion tracking performance in the presence of complex external disturbances [14]. Newton analyzed the difference of control theory and control effects between neural network control algorithm with the traditional PID control algorithm in motor and valve control cylinder valve-controlled system [15]. Yao concerned the high dynamic tracking control of hydraulic servo systems and found the proposed feedback linearization controller guarantees more excellent tracking performance even with high-frequency tracking demand than the proportional-integral controller and the proportional-integral controller [16].

Provided the capacity of parameter adaptability and good robustness for nonlinear control system, sliding mode control has become increasingly applicable to electrohydraulic servo systems control. Mohseni et al. presented a decoupled sliding mode with fuzzy neural network controller for a nonlinear system, which can make the response of system converge faster [17]. Perron et al. presented a sliding mode controller to resolve efficiency variations of the pump which are dependent on the pressure operating point and its speed of rotation [18].

It is easy to see that the application of advanced control theory has been a significant research direction for modern hydraulic control [19–23]. However, it is more challenging for the speed control system facing the flexible load. For example, a sliding mode control algorithm based on fuzzy reaching law for the underwater vehicle under hydraulic flexible traction system with low rigidity and variable load was designed by Zhao et al. [24]. Zhao presented a loop-type traction system with one hydraulic winch differing from the open-type towing system with double hydraulic winches which increased the complexity and difficulty of control system.

For the research object of the paper, it is a novel kind of underwater flexible towing system depending on two hydraulic valve-controlled motor winches and the wire rope. The mathematical model of the open-type hydraulic flexible towing system must be rebuilt in view of nonlinear flexible wire rope, hydraulic valve-controlled motor, the vehicle features, and the water resistance force in a limited pool. Thus, it is meaningful to design a novel sliding mode control arithmetic for the open-type hydraulic flexible towing system.

This article is organized as follows: the Problem Statement describes the problem formulation. The model of the underwater vehicle towing system including the valve-controlled hydraulic motor driving device, the wire rope traction mechanism, and the vehicle body is discussed in the Modeling of Underwater Vehicle Control System. Then, the speed

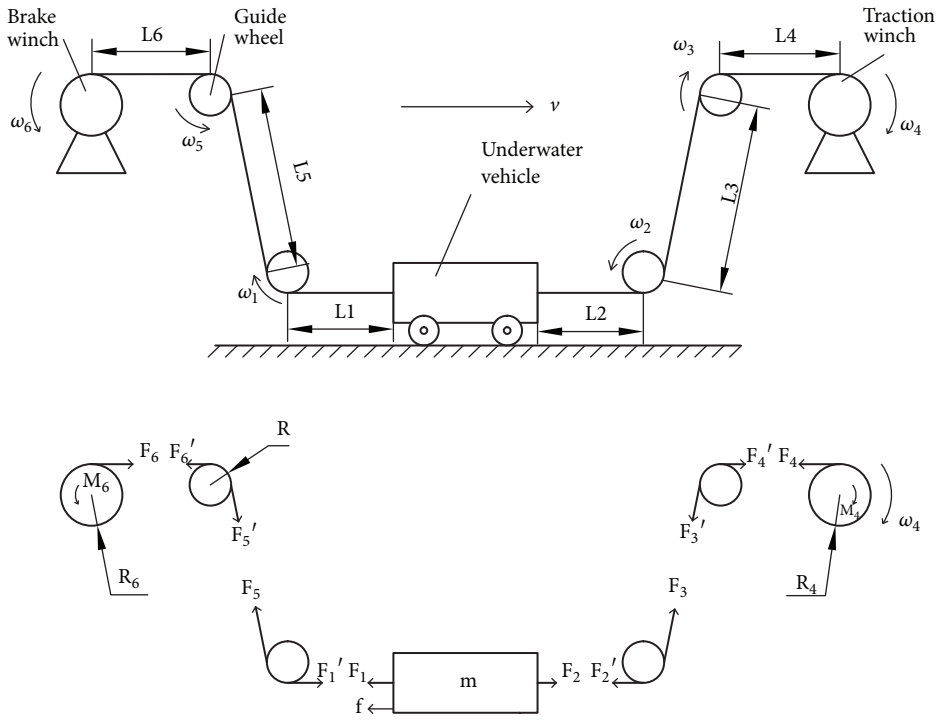

Figure 2: Schematic diagram of underwater vehicle propelled by hydraulic winch.

controller taking advantage of fast terminal sliding mode method is developed in the Research on Fast Terminal Sliding Mode Control. Next, in the Simulation and Discussion, the robustness and effectiveness of the presented control laws are confirmed by Matlab/Simulink. The satisfactory dynamic quality of the control system is evidenced by comparing the simulations in the disturbance and interference-free environment. And the physical controller is verified by the use of the semiphysical simulation platform in the Semiphysical Simulation. Finally, a brief conclusion is included in the Conclusion.

2. Problem Statement

Since the effective length of the track is only 10.5 meters, the wheeled vehicle which has great mass need be controlled to accelerate to specific speed firstly, keep uniform running for several seconds stably, and decelerate gradually to 0 m/s lastly. Under these circumstances, the speed control system of the underwater wheeled vehicle must have short rising time, veracity, and anti-interference ability to conquer the strong coupling, nonlinear, time-varying load, and environmental constraints of the towing system.

In addition, the speed controller should actually output two valve opening control signals at the same time, where one is for the traction winch and another one is for the brake winch. It is essential to put forward multimode synchronous control strategy which can reduce the tensile impact of wire rope while the underwater wheeled vehicle begins to slow down from constant speed.

3. Modeling of Underwater Vehicle Control System

3.1. Modeling of Flexible Traction System. Figure 2 is the force analysis diagram of the underwater wheeled vehicle towing system. As exhibited in this figure, we assume that the direction of motion of the winches and pulleys is positive direction. And the angular velocity of the brake winch, pulleys, and the traction winch is defined respectively as ω_1, ω_2, ω_3, ω_4, ω_5, and ω_6. Owing to the arrangement of the hydraulic winches, chain wheels, and the underwater vehicle, the wire rope can be segmented into six sections (L1, L2, L3, L4, L5, and L6). For convenience, the tension of each part is defined separately as F_1, F_2, F_3, F_4, F_5, and F_6. The resultant force of the underwater wheeled vehicle consists of three forces, that is, the front traction force F_2, posterior force F_1, and resisting force f.

On the basis of the force analysis, we can acquire the kinetic equation of the underwater wheeled vehicle as follows.

$$F_2 - F_1 - f = M\frac{dV_L}{dt} \tag{1}$$

where F_1 stands for the tensile force of segment L1 on the back of the vehicle, F_2 stands for the tensile force of the first segment L2 in the front of the vehicle, f is water resistance force which is applied on the vehicle, M is the mass of the underwater vehicle, and V_L is the running velocity of the underwater vehicle.

Owing to the nonlinear characteristic of the wire rope and the coupling of the applied forces from two directions, it is necessary for us to analyze tension of steel wire rope which is critically important element in this open-type flexible towing

system. The mechanical model of unrelaxed rope can be described as the Kelvin-Voigt model. And the tensile force becomes zero when the rope is slack. Under the condition of stretching, the deformation quantity of each segment is expressed as Δx_i (i = 1, 2, 3, 4, 5, 6), respectively.

Taking two states of the wire rope into account, the tensile force of each rope segment can be described as follows.

$$F_i = \begin{cases} k_i \Delta x_i + c_i \Delta \dot{x}_i, & \Delta x_i > 0 \\ 0, & \Delta x_i \le 0 \end{cases} \tag{2}$$

Six rope segments share the same parameters, elasticity modulus $k = k_1 = k_2 = k_3 = k_4 = k_5 = k_6$, viscous modulus $c = c_1 = c_2 = c_3 = c_4 = c_5 = c_6$. Considering the moving condition, the dynamical elongations of each part of rope can be expressed as follows.

$$\begin{aligned} \Delta x_1 &= X_L + \int \omega_1 dt \cdot R \\ \Delta x_2 &= \int \omega_2 dt \cdot R - X_L \\ \Delta x_3 &= \int \omega_3 dt \cdot R - \int \omega_2 dt \cdot R \\ \Delta x_4 &= \int \omega_4 dt \cdot R_4 - \int \omega_3 dt \cdot R \\ \Delta x_5 &= \int \omega_5 dt \cdot R - \int \omega_1 dt \cdot R \\ \Delta x_6 &= \int \omega_6 dt \cdot R - \int \omega_5 dt \cdot R_6 \end{aligned} \tag{3}$$

where X_L is the running distance of vehicle. Consider the steady condition, the hydraulic winch, and guide wheel have equal linear speed, $w_1 \cdot R = w_2 \cdot R = w_3 \cdot R = w_4 \cdot R_4 = w_5 \cdot R = w_6 \cdot R_6$. Using the Laplace transformation, we can get

$$\begin{aligned} \Delta x_1(s) \cdot s &= V_L(s) + \omega_1(s) \cdot R \\ \Delta x_2(s) \cdot s &= \omega_2(s) \cdot R - V_L(s) \\ \Delta x_3(s) \cdot s &= \omega_3(s) \cdot R - \omega_2(s) \cdot R \\ \Delta x_4(s) \cdot s &= \omega_4(s) \cdot R_4 - \omega_3(s) \cdot R \\ \Delta x_5(s) \cdot s &= \omega_5(s) \cdot R - \omega_1(s) \cdot R \\ \Delta x_6(s) \cdot s &= \omega_6(s) \cdot R_6 - \omega_5(s) \cdot R \end{aligned} \tag{4}$$

When the underwater vehicle is doing accelerated movement, the posterior force which is a resistance should be as small as possible for the rapidity of speed control. Based on the multimode synchronous control strategy, F1 can be regarded as zero. Combining (1) and (2), we can get the kinetic equation simplified as follows.

$$F_2 - f = k_2 \cdot \Delta x_2 + c_2 \cdot \Delta \dot{x}_2 - f = M \cdot \dot{V}_L \tag{5}$$

Equation (6) can be written as

$$k_2 \cdot \Delta x_2(s) + c_2 \cdot \Delta x_2(s) \cdot s = M \cdot V_L(s) \cdot s + f \tag{6}$$

Substituting (4) in (6) results in

$$\begin{aligned} &k_2 \omega_2(s) R - k_2 V_L(s) + c_2 \omega_2(s) R \cdot s - c_2 V_L(s) \cdot s \\ &\quad = M V_L(s) \cdot s^2 + f \cdot s \end{aligned} \tag{7}$$

In the open-style flexible towing system, the relationship about the underwater vehicle velocity, water resistance, and hydraulic winch rotational speed can be extrapolated as follows.

$$V_L(s) = \frac{\omega_4(s) \cdot (k + cs) \cdot R_4 - f \cdot s}{Ms^2 + cs + k} \tag{8}$$

3.2. Modeling of Hydraulic Winch System. In order to allow the transfer function of the hydraulic winch, three fundamental equations consisting of the hydraulic actuated valve flow equation, hydraulic motor flow rate continuation equation, and the motor torque balance equation must be set out. And their Laplace transform can be written as follows.

$$\begin{aligned} Q_L &= K_q X_V - K_c P_L \\ Q_L &= D_m s \theta_m + C_{tm} P_L + \frac{V_m}{4\beta_e} s P_L \\ T_s &= P_L D_m = J_m s^2 \theta_m + B_m s \theta_m + G \theta_m + T_L \end{aligned} \tag{9}$$

where T_s is the theoretical torque generated by hydraulic motor. K_q is the flow gain of the valve. K_c is the flow pressure coefficient. D_m is the displacement of the hydraulic motor. C_{tm} is the total leakage factor of the hydraulic motor. V_m is the total volume of the pipe. β_e is the oil elasticity modulus. J_m is the inertia reflected to the rotation shaft of hydraulic motor. B_m is the viscous damping coefficient of load and hydraulic motor. G is the load torsion spring stiffness. And T_L is the external load torque acting on the motor shaft.

By putting these three fundamental equations together and eliminating the middle term, the transform function of the valve opening degree and vehicle speed comes out as follows [25].

$$\begin{aligned} \dot{\theta}_m &= \frac{\left(K_q / D_m\right) x_v - \left(1 / D_m^2\right)\left(K_{ce} + \left(V_m / 4\beta_e\right) s\right) T_L}{s^2 / \omega^2{}_h + \left(2\xi_h / \omega_h\right) s + 1 + B_m K_{ce} / D_m^2} \\ \omega_h &= \sqrt{\frac{4\beta_e D_m^2}{V_m J}} \\ \xi_h &= \frac{K_{ce}}{D_m}\sqrt{\frac{\beta_e J}{V_m}} + \frac{B_m}{4D_m}\sqrt{\frac{V_m}{\beta_e J}} \\ K_{ce} &= K_c + C_{tm} \end{aligned} \tag{10}$$

where ω_h is equivalent hydraulic natural frequency. ζ_h is damping ratio of hydraulic valve-controlled motor. And K_{ce} is general coefficient of flow pressure.

3.3. Modeling of External Load. The force analysis of the open flexible traction structure is described as shown in Figure 2.

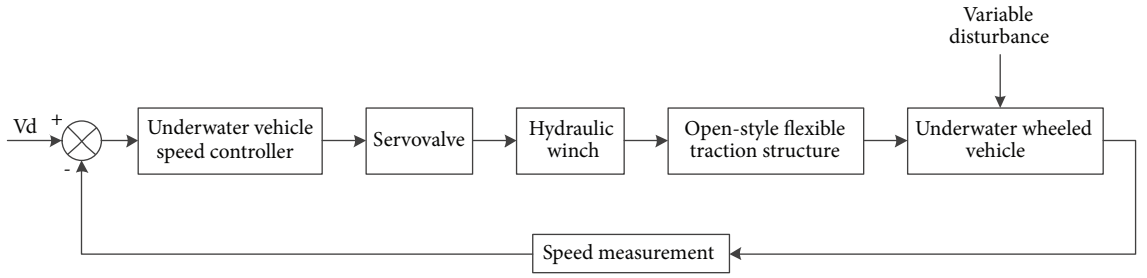

Figure 3: Speed control of the underwater vehicle.

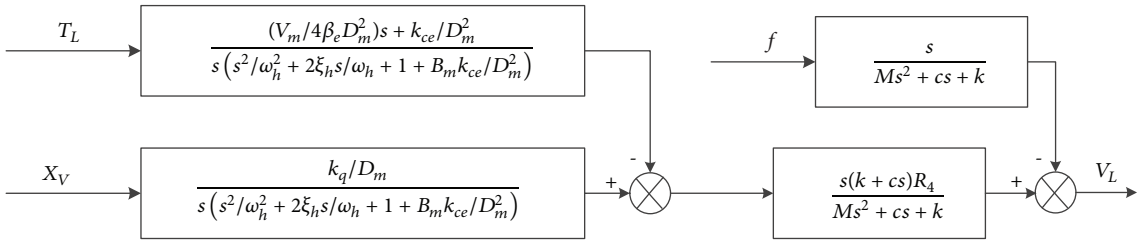

Figure 4: The transfer function diagram of the underwater vehicle speed control system.

According to the torque equilibrium equation of winch, we can get the following.

$$T_L = R_4 \cdot \sum_{i=2}^{4} \left(K_i \Delta X_i + C_i \Delta \dot{X}_i\right) \tag{11}$$

Combining (4), (8), and (11), the torque equilibrium equation of hydraulic may be obtained as follows.

$$\begin{aligned} T_L &= R_4 \left[k \frac{\omega_4 R_4 - V_L}{s} + c\left(\omega_4 R_4 - V_L\right)\right] \\ &= R_4 \left[\frac{kR_4 + cR_4 s}{s}\omega_4 - \frac{k + cs}{s} V_L\right] \\ &= R_4 MsV_L + R_4 f \end{aligned} \tag{12}$$

The model of water resistance force applied on the underwater vehicle can be expressed as follows [26].

$$f = 0.5 C_d \rho A V_L^2 \tag{13}$$

3.4. Modeling of the Underwater Vehicle Speed Control System. As we can know from Figure 3, according to the deviation between the measured velocity and the given value, the speed controller of underwater wheeled vehicle computes the opening degree of valve and outputs the control signal to the servo valve. And, then, the rotating winch drives the open-type flexible towing structure under the variable disturbance.

Integrating each of the component transfer functions (8), (10), (12), and (13), we can acquire the transfer function structure diagram of the whole hydraulic flexible towing speed control system which is shown; the transfer function diagram of the underwater vehicle speed control system may be obtained in Figure 4.

Different from the traditional hydraulic speed servo control system, the underwater wheeled vehicle flexible towing system utilizes the steel wire rope as the traction medium, which increases the system order and reduces the system rigidity. In addition, compared with the conventional hydraulic winch, the external load is time-varying owing to the variable vehicle speed and water resistance, which brings great challenges for the stability speed control.

In order to calculate the transfer function expression for the running velocity and the opening of the servo-proportional control valve, we have to simplify the above transfer function diagram. For the sake of convenience, the substitution variables are defined as follows.

$$\begin{aligned} A &= \frac{k_q/D_m}{s\left(s^2/\omega_h^2 + 2\xi_h s/\omega_h + 1 + B_m k_{ce}/D_m^2\right)} \\ B &= \frac{\left(V_m/4\beta_e D_m^2\right)s + k_{ce}/D_m^2}{s\left(s^2/\omega_h^2 + 2\xi_h s/\omega_h + 1 + B_m k_{ce}/D_m^2\right)} \\ C &= \frac{s\left(k + cs\right)R_4}{Ms^2 + cs + k} \\ D &= \frac{s}{Ms^2 + cs + k} \end{aligned} \tag{14}$$

On the basis of the above equation, we can acquire

$$\begin{aligned} v_L(s) &= \left(AX_V(s) - BT_L(s)\right)C - Df(s) \\ &= ACX_V(s) - BC\left(R_4 Msv(s) + R_4 f\right) - Df(s) \\ &= ACX_V(s) - BCR_4 Msv(s) \\ &\quad - \left(BCR_4 - D\right)f(s) \end{aligned} \tag{15}$$

where $X_V(s)$ is the control input of servo-proportional control valve, $v(s)$ is the running velocity of the underwater wheeled

vehicle on last measuring period, and f(s) is the water resistance acting on the vehicle.

4. Research on Fast Terminal Sliding Mode Control

It is difficult to pinpoint the mathematical model of the underwater vehicle speed control system on account of the large inertia, variable load, time delay, parameter uncertainty, and strong nonlinearity features. When the vehicle moves in the limited rectangular parallelepiped pond, the existing fluid-structure interaction, the pond wall effect, the fluid resistance, and the change of system state usually make the system deviate from the design state.

Sliding mode control has received wide attention and research because of its good robustness to the external disturbance and parameter perturbation. On its basis, the terminal sliding mode control theory introduces nonlinearity into the design of sliding mode which brings about the limited time convergence, rapid convergence, and stronger robustness. Therefore, it is suitable for the underwater vehicle speed control system.

Taking a SISO second-order nonlinear system as the research object,

$$\begin{aligned} \dot{x_1} &= x_2 \\ \dot{x_2} &= f(x) + g(x)\,u + d(t) \end{aligned} \tag{16}$$

The system state is expressed as $x = [x_1 \quad x_2]$, f(x) and g(x) are the known smooth functions, respectively, $g(x) \neq 0$, and d(t) denotes the uncertainty and disturbance satisfied with $|d(t)| \leq L$.

A fast terminal sliding surface is selected as follows.

$$s_1 = \dot{s_0} + a_0 s_0 + \beta_0 s_0^{q_0/p_0} \tag{17}$$

where $\alpha_0, \beta_0 > 0$ and $q_0, p_0 (q_0 < p_0)$ are positive odd numbers, $s_0 = x_1$. The linear term $\alpha_0 s_0$ is involved to optimize the rapidity of the approaching area, and the nonlinear term $\beta_0 s_0^{q_0/p_0}$ can ensure that the system motion points can converge to the sliding surface in finite time [27].

Next, according to the concept and function of reaching law which can ensure the excellent dynamic quality of the system states in the approaching area, the fast terminal reaching function is devised as follows [28].

$$\dot{s_1} = -\phi s_1 - \gamma s_1^{q/p} - d(t) \tag{18}$$

where $\gamma, \emptyset > 0$, $p, q > 0$ are positive odd numbers. In the fast terminal reaching law, it makes sure that the system can get to the sliding surface $s_1(x) = 0$ from any initial state in a finite time to use the item with fractional diffusion power instead of the sign function. In addition, differing from the conventional reaching law, the fast terminal reaching law without the discontinuous items can reduce the chatting caused by the sign function efficaciously.

Table 1: Parameters of the hydraulic flexible towing system.

Parameter name	Note	Unit	value
Winch radius	R_4	*m*	*0.27*
Valve flow gain	K_q		*0.1193*
Motor leakage factor	C_{tm}		1.45×10^{-12}
Charge oil pressure	P_s	*MPa*	*23*
Motor displacement	D_m	m^3/rad	*0.00207*
Volume of cavity	V_m	m^3	*0.04*
Bulk modulus of hydraulic	β_e	*Pa*	7.0×10^8
Flow-pressure coefficient	K_{ce}	$m^5/(Ns)$	4.54×10^{-12}
Vehicle quality	*M*	*kg*	*20000*
Meeting area of flowing	*A*	m^2	*16.8*

The following formula is derived.

$$\begin{aligned} \dot{s_1} &= \ddot{s_0} + \alpha_0 \dot{s_0} + \beta_0 \frac{d}{dt} s_0^{q_0/p_0} \\ &= -f(x) - g(x)\,u + \alpha_0 \dot{s_0} + \beta_0 \frac{d}{dt} s_0^{q_0/p_0} \end{aligned} \tag{19}$$

Combining (19) with (18), the fast sliding mode controller is developed as

$$\begin{aligned} &u(t) \\ &= -g(x)^{-1} \left(f(x) + \alpha_0 \dot{s_0} - \beta_0 \frac{d}{dt} s_0^{q_0/p_0} - \phi s_1 - \gamma s_1^{q/p} \right) \end{aligned} \tag{20}$$

The Lyapunov function is selected as

$$V = \frac{1}{2} s_1^2 \tag{21}$$

With reference to (17) and (18),

$$\dot{V} = s_1 \dot{s_1} = -\phi s_1^2 - \gamma s_1^{(p+q)/p} - s_1 d(t) \tag{22}$$

We know that (p + q) is an even number, because $-\gamma s_1^{(p+q)/p} - s_1 d(t) \leq 0$ is satisfied; i.e., $\gamma \geq |1/s_1^{q/p}||d(t)|$ or $\gamma \geq |1/s_1^{q/p}|L$; therefore, we have $\dot{V} \leq 0$.

5. Simulation and Discussion

In this section, the model of the underwater wheeled vehicle towing system is simplified firstly, and the velocity controller on account of the fast terminal sliding mode control theory is designed. To examine the performance of the velocity controller, the whole-course towing movement simulations based on the FTSMC and PID controller have been both carried out in Matlab/Simulink platform.

5.1. Model Simplification. On the basis of the actual equipment selection, the main nominal parameters of the hydraulic flexible towing system are exhibited in Table 1.

According to the main system parameters, the transfer function diagram of the underwater wheeled vehicle speed control system may then be acquired in Figure 5.

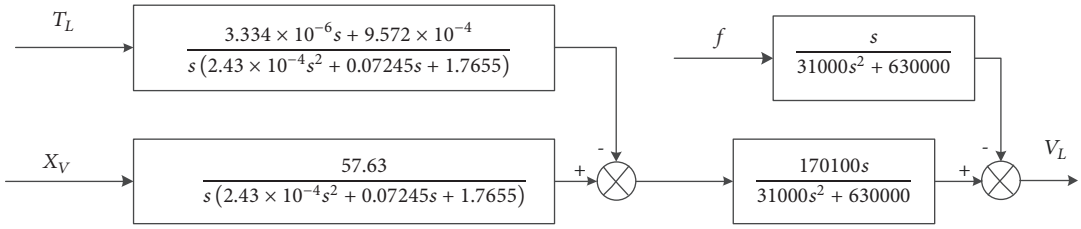

Figure 5: The transfer function diagram of the underwater vehicle speed control system.

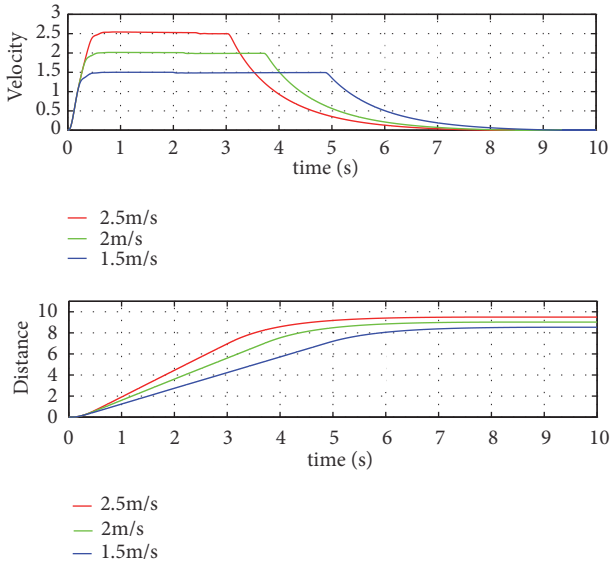

Figure 6: Motion curve based on PID control law.

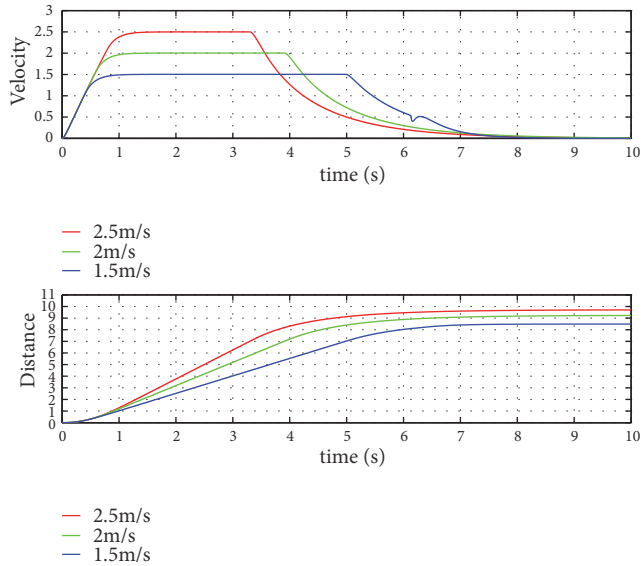

Figure 7: Motion curve based on LSM control law.

After simplification, the transfer function of the underwater vehicle speed control system may be written as

$$v_L(s) = \frac{178.4688}{s^2 + 0.826244s + 20.26594} X_V(s) - \frac{24.81859s}{s^2 + 0.826244s + 20.26594} v(s) - \frac{3.2168 \times 10^{-5}s^2 + 8.0147 \times 10^{-4}}{s^2 + 0.826244s + 20.26594} f(s) \quad (23)$$

The status parameters of the underwater wheeled vehicle velocity control system can be selected as $x_1 = V_L$ and $x_2 = \dot{x}_1$. Then the state-space equation of the hydraulic flexible towing system can be obtained as follows.

$$\begin{aligned} x_1 &= V_L \\ \dot{x}_1 &= x_2 \\ \dot{x}_2 &= -20.26594x_1 - 0.826244x_2 + 178.4688u \\ &\quad - 24.81859\dot{v} - 3.2188 \times 10^{-5}\ddot{f} - 8.0147 \\ &\quad \times 10^{-4}\dot{f} \end{aligned} \quad (24)$$

where v is the running velocity of the underwater wheeled vehicle on last measuring period, and f is the water resistance acting on the vehicle.

5.2. Comparing Simulation with Multiple Given Speeds. In this part, the PID control method has been realized firstly in the simulation platform with the following control parameters: P=2, I=0.8, and D=0.1.

As shown in Figure 6, the entire journey movement simulations with three different inputs 2.5 m/s, 2 m/s, and 1.5 m/s, respectively, are experimented. Using the PID approach, the practical uniform velocity can catch up with the given speed in an acceptable time; however the steady-state deviation of the uniform phase increases with the set velocity. In addition, there is just a small margin for the track length when the set speed is 2.5 m/s, which means there is a risk of hitting the pool wall.

After that, the classical line sliding mode control method is applied to the design of the speed controller. And the simulation has been carried out, as shown in Figure 7.

Thirdly, the FTSMC method is realized secondly in the simulation platform with the following control parameters: $\alpha_0 = 20$, $\beta_0 = 0.1$, $q_0 = 5$, $p_0 = 7$, $\varphi = 1400$, $\gamma = 100$, $q = 3$, and $p = 5$, as shown in Figure 8.

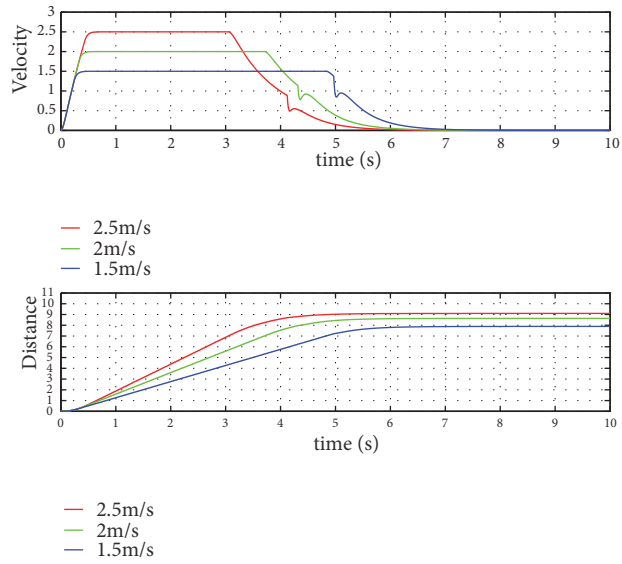

Figure 8: Motion curve based on FTSMC control law.

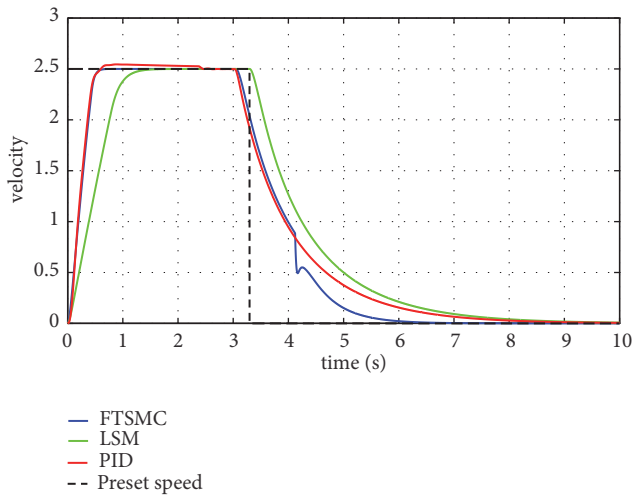

Figure 9: Comparing velocity curve.

In the next step, the comparing diagram putting the PID curve, LSM curve, and the FTSMC curve together is shown in Figures 9 and 10.

As shown in Figure 8, using the FTSMC approach, the practical uniform velocity can also catch up with the given speed in an acceptable time, and the steady-state accuracy of the uniform phase is excellent. In addition, there is still a big margin for the track length when the set speed is 2.5 m/s. With the analysis of the comparing motion curve, the control effect of two controllers can meet the experiment requirements, and the FTSMC controller is more excellent.

5.3. Comparing Simulation with Parameter Perturbation. A comparison experiment referring to multiple parameter perturbations is carried out to examine the adaptable character of the FTSMC controller we designed, as shown in Figure 11.

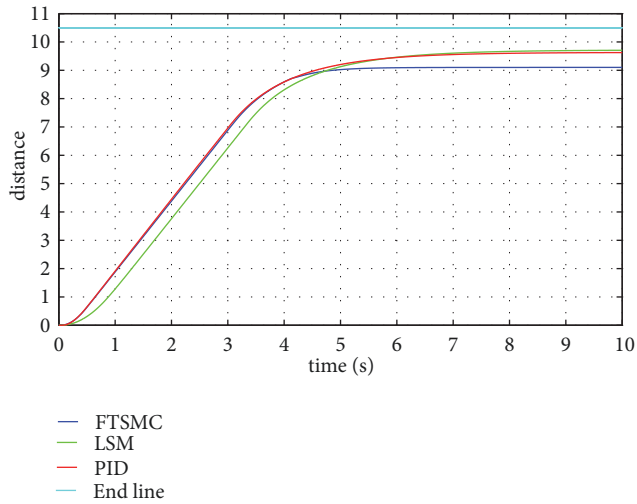

Figure 10: Comparing distance curve.

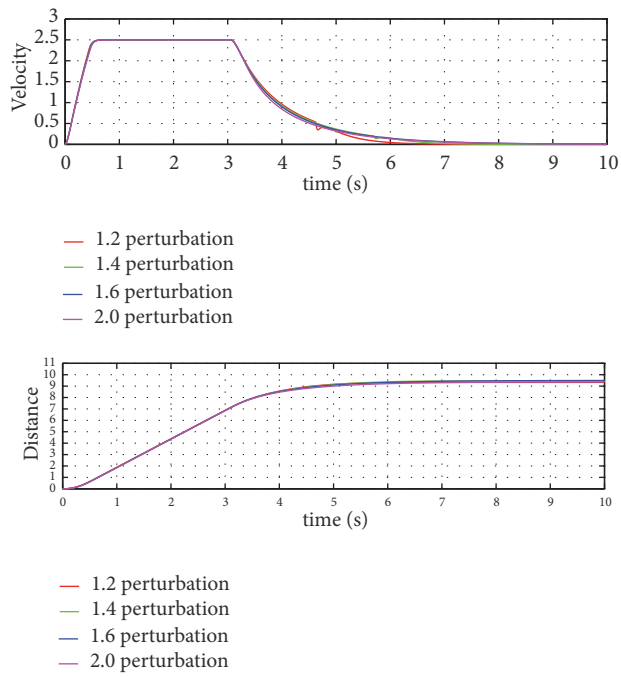

Figure 11: FTSMC control simulation with parameter perturbation.

In this part, the FTSMC control method has been realized in the simulation platform with the 1.2, 1.4, 1.6, and 2 times of water resistance coefficient.

Exhibited in Figure 11, using the FTSMC approach, the practical velocity of the uniform phase can keep stable as well as accuracy under multiple coefficients, which displays that the speed controller of the underwater wheeled vehicle can be adaptable to the different parameter perturbations.

To examine the performance of the multimode synchronous control strategy, the entire journey movement simulations have been carried out in Matlab/Simulink, as shown in Figure 12.

5.4. Comparing Simulation with Impulsive Disturbance. A comparison experiment referring to impulsive disturbance is

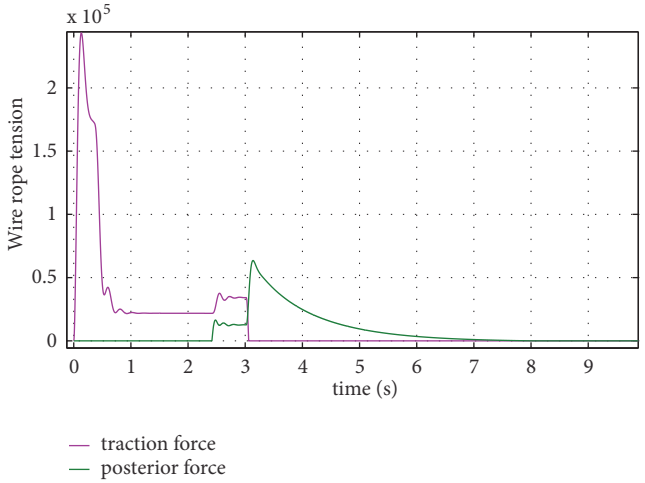

Figure 12: Wire rope tension curve.

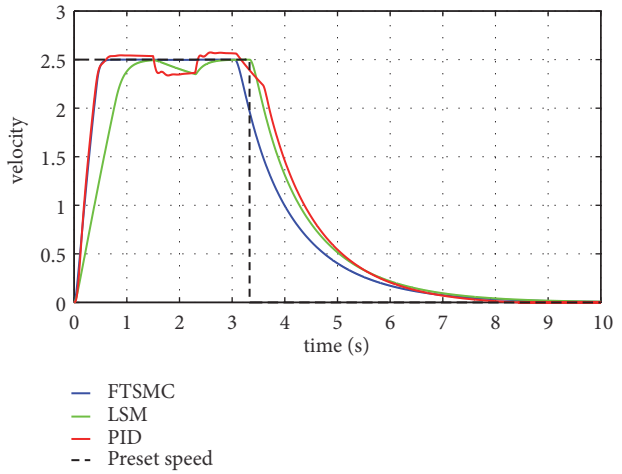

Figure 13: Comparing velocity curve with impulsive disturbance.

carried out to examine the robust character of the FTSMC controller we designed, as shown in Figures 13 and 14.

In this part, the FTSMC control method has been realized in the simulation platform with impulsive disturbance which is applied to the wheeled vehicle in the negative direction and is maintained for 0.8 seconds.

The velocity response of the FTSMC controller still can converge to the desired speed. However the speed responses of PID and LSM controllers appear with a fluctuation, and the distances of the vehicle have crossed the end line of the track.

6. Semiphysical Simulation

After the real control equipment manufactured, a semiphysical simulation platform based on Matlab/Simulink and VxWorks real-time system is set up, which connects physical controller with simulator by the authentic electrical interface and communication, as shown in Figure 15. The controller outputs the opening signal of the valve to the target simulator running the dynamic mathematic model instead of the

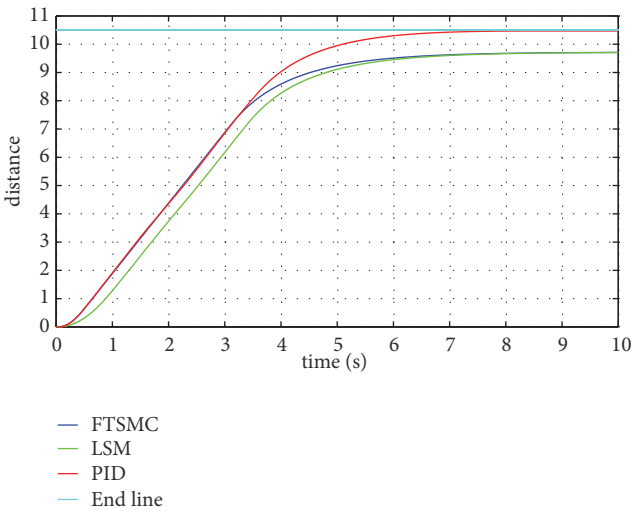

Figure 14: Comparing distance curve with impulsive disturbance.

Figure 15: Semiphysical simulation platform.

physical control object. And the entire journey movement experiment of the underwater wheeled vehicle has been carried out by use of the semiphysical simulation platform, as shown in Figure 16.

During the entire journey movement experiment, the velocity and distance response of the underwater wheeled vehicle still behaves well on the function of the practical controller based on the FTSMC theory.

7. Conclusion

In this paper, we introduced an underwater wheeled vehicle flexible towing system. After analyzing each component characteristic of the underwater wheeled vehicle towing system, the dynamic mathematical system model is established. Aiming at the environmental constraint and disturbance caused by the external environment, the fast terminal sliding mode variable structure controller is designed. At last, effective simulations based on the semiphysical simulation platform is carried out. Analyzing the simulation results, the velocity and displacement converge to the desired status rapidly which indicates that the speed control system based on the FTSMC theory can be robust against the nonlinear, environmental disturbance.

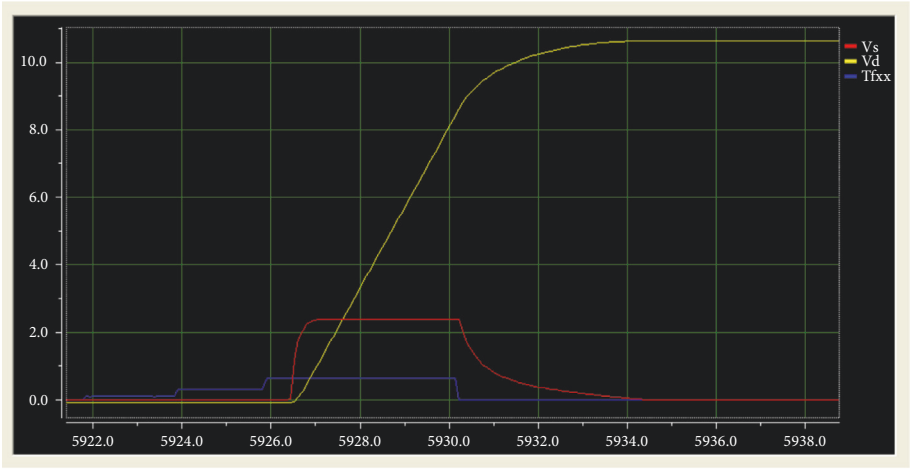

Figure 16: Semiphysical simulation.

Data Availability

The data used to support the findings of this study are available from the corresponding author upon request.

Disclosure

The authors received no financial support for the research, authorship, and/or publication of this article.

Conflicts of Interest

The authors declare that they have no conflicts of interest.

References

[1] Y. Xia, G. Xu, K. Xu, Y. Chen, X. Xiang, and Z. Ji, "Dynamics and control of underwater tension leg platform for diving and leveling," *Ocean Engineering*, vol. 109, pp. 454–478, 2015.

[2] Y. Xia, K. Xu, Y. Li, G. Xu, and X. Xiang, "Modeling and Three-Layer Adaptive Diving Control of a Cable-Driven Underwater Parallel Platform," *IEEE Access*, vol. 6, pp. 24016–24034, 2018.

[3] L. Pugi, B. Allotta, and M. Pagliai, "Redundant and reconfigurable propulsion systems to improve motion capability of underwater vehicles," *Ocean Engineering*, vol. 148, pp. 376–385, 2018.

[4] G. Liu, X. Shen, G. H. Xu, S. R. Xun, and Z. Chen, "Motion Control of an Underwater Wheeled Vehicle in Constrained Pond," in *Proceedings of the OCEANS 2017*, vol. 8, Anchorage, Ala, USA, 2017.

[5] B. Jin, *Study on the Fuzzy Sliding Mode Control Method of Electrohydraulic Position Servo Control System [Ph.D. thesis]*, Taiyuan University of Technology, Taiyuan, China, 2010.

[6] L. Pugi, E. Galardi, G. Pallini, L. Paolucci, and N. Lucchesi, "Design and testing of a pulley and cable actuator for large ball valves," *Proceedings of the Institution of Mechanical Engineers, Part I: Journal of Systems and Control Engineering*, vol. 230, no. 7, pp. 622–639, 2016.

[7] X. Xiang, C. Yu, and Q. Zhang, "On intelligent risk analysis and critical decision of underwater robotic vehicle," *Ocean Engineering*, vol. 140, pp. 453–465, 2017.

[8] X. B. Xiang, L. Lapierre, and B. Jouvencel, "Smooth transition of AUV motion control: from fully-actuated to under-actuated configuration," *Robotics and Autonomous Systems*, vol. 67, pp. 14–22, 2015.

[9] N. Wang, J.-C. Sun, M. Han, Z. Zheng, and M. J. Er, "Adaptive approximation-based regulation control for a class of uncertain nonlinear systems without feedback linearizability," *IEEE Transactions on Neural Networks and Learning Systems*, vol. 29, no. 8, pp. 3747–3760, 2018.

[10] N. Wang, S. Lv, W. Zhang, Z. Liu, and M. J. Er, "Finite-time observer based accurate tracking control of a marine vehicle with complex unknowns," *Ocean Engineering*, vol. 145, pp. 406–415, 2017.

[11] N. Wang, S. Su, J. Yin, Z. Zheng, and M. J. Er, "Global Asymptotic Model-Free Trajectory-Independent Tracking Control of an Uncertain Marine Vehicle: An Adaptive Universe-Based Fuzzy Control Approach," *IEEE Transactions on Fuzzy Systems*, vol. 26, no. 3, pp. 1613–1625, 2018.

[12] J. Peng, S. Li, and Y. Fan, "Modeling and Parameter Identification of the Vibration Characteristics of Armature Assembly in a Torque Motor of Hydraulic Servo Valves under Electromagnetic Excitations," *Advances in Mechanical Engineering*, vol. 2014, 10 pages, 2014.

[13] Q. Chen, W. Li, X. H. Wang, and J. C. Yu, "Development of a dynamic model for a constant tension winch," in *Proceedings of the OCEANS 2015-MTS/IEEE*, Washington, DC, USA, 2015.

[14] J. Wei, Q. Zhang, M. Li, and W. Shi, "High-performance motion control of the hydraulic press based on an extended fuzzy disturbance observer," *Proceedings of the Institution of Mechanical Engineers, Part I: Journal of Systems and Control Engineering*, vol. 230, no. 9, pp. 1044–1061, 2016.

[15] D. A. Newton, "Application of a neural network controller to control a rotary drive system with high power efficiency," in *Proceedings of the 7th Bath International Fluid Power Workshop, Innovations in Fluid Power*, pp. 41–54, 1995.

[16] J. Yao, G. Yang, and Z. Jiao, "High dynamic feedback linearization control of hydraulic actuators with backstepping," *Proceedings of the Institution of Mechanical Engineers, Part I:*

Journal of Systems and Control Engineering, vol. 229, no. 8, pp. 728–737, 2015.

[17] S. A. Mohseni, M. A. Shooredeli, and M. Teshnehlab, "Decoupled sliding-mode with fuzzy neural network controller for EHSS velocity control," in *Proceedings of the International Conference on Intelligent and Advanced Systems (ICIAS '07)*, pp. 7–11, IEEE, Kuala Lumpur, Malaysia, November 2007.

[18] M. Perron, J. De Lafontaine, and Y. Desjardins, "Sliding-mode control of a servomotor-pump in a position control application," in *Proceedings of the Canadian Conference on Electrical and Computer Engineering*, pp. 1287–1291, Saskatoon, Canada, May 2005.

[19] N. Wang, J.-C. Sun, and M. J. Er, "Tracking-error-based universal adaptive fuzzy control for output tracking of nonlinear systems with completely unknown dynamics," *IEEE Transactions on Fuzzy Systems*, vol. 26, no. 2, pp. 869–883, 2018.

[20] N. Wang, Z. Sun, J. Yin, S.-F. Su, and S. Sharma, "Finite-Time Observer Based Guidance and Control of Underactuated Surface Vehicles with Unknown Sideslip Angles and Disturbances," *IEEE Access*, vol. 6, pp. 14059–14070, 2018.

[21] X. Xiang, C. Yu, J. Zheng, and G. Xu, "Motion forecast of intelligent underwater sampling apparatus — Part I: Design and algorithm," *Indian Journal of Geo-Marine Sciences*, vol. 44, no. 12, pp. 1962–1970, 2015.

[22] N. Wang, Z. Sun, Z. Zheng, and H. Zhao, "Finite-time sideslip observer-based adaptive fuzzy path-following control of underactuated marine vehicles with time-varying large sideslip," *International Journal of Fuzzy Systems*, vol. 20, no. 6, pp. 1767–1778, 2018.

[23] N. Wang, Y. Gao, Z. Sun, and Z. Zheng, "Nussbaum-based adaptive fuzzy tracking control of unmanned surface vehicles with fully unknown dynamics and complex input nonlinearities," *International Journal of Fuzzy Systems*, vol. 20, no. 1, pp. 259–268, 2018.

[24] Y. Zhao, Y.-K. Xia, Y. Chen, and G.-H. Xu, "A Speed Control Method for Underwater Vehicle under Hydraulic Flexible Traction," *Journal of Control Science and Engineering*, vol. 2015, 16 pages, 2015.

[25] T. L. Chang, *Hydraulic Control System*, Tsinghua University Press, Beijing, China, 2014.

[26] G. X. Hou, J. L. Sun, X. Z. Wang, and D. K. Feng, *Engineering Fluid Mechanics*, China Machine Press, Beijing, China, 2006.

[27] G. Liu, G. Xu, Y. Chen, W. Zhang, G. Wang, and F. Li, "A novel terminal sliding mode control for the navigation of an underactuated UUV," in *Proceedings of the 26th Annual International Ocean and Polar Engineering Conference, ISOPE 2016*, pp. 603–610, Greece, July 2016.

[28] J. Liu and X. Wang, *Advanced Sliding Mode Control for Mechanical Systems: Design, Analysis and Matlab Simulation*, Tsinghua University Press, 2011.

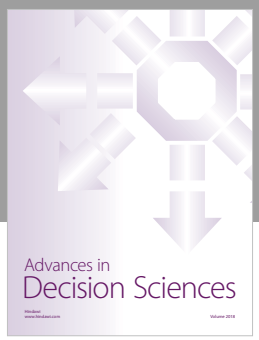

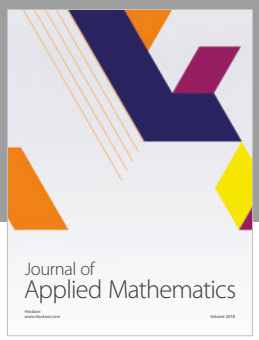

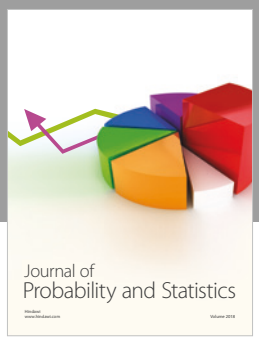

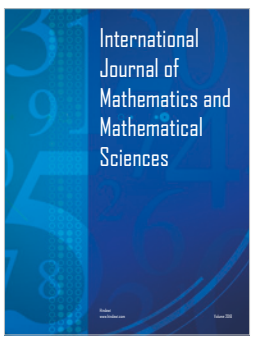

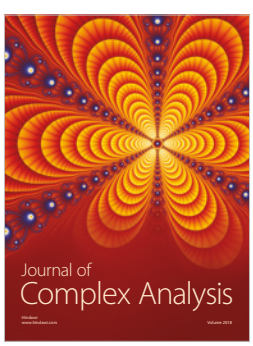

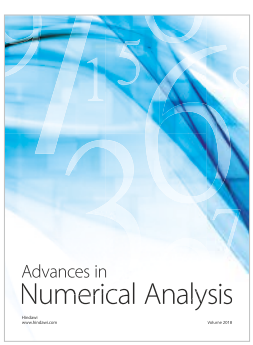

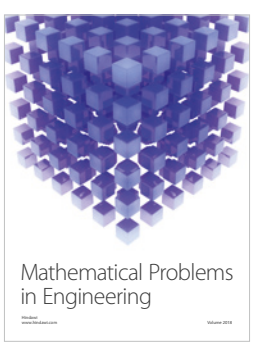

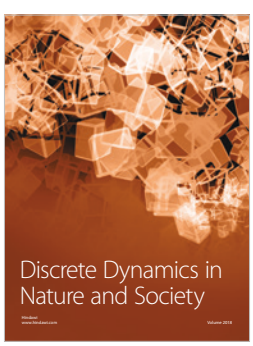

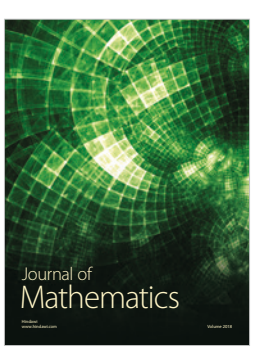

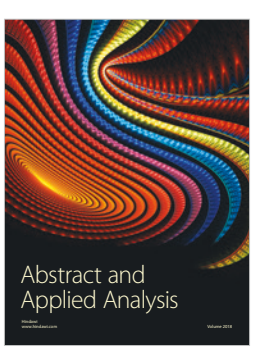

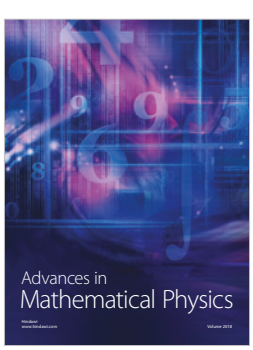

Hindawi

Submit your manuscripts at
www.hindawi.com